Optimized Methodology for Neonatal Diffusion Tensor Imaging Processing and Study-specific Template Construction*

Iordanis E. Evangelou[1,3], Ahmed Serag[1], Marine Bouyssi-Kobar[1,3], Adre J. du Plessis[2,3] and Catherine Limperopoulos[1,2,3]

Abstract— **Diffusion tensor imaging (DTI) has been widely used to study cerebral white matter microstructure in vivo. There is a plethora of open source tools available to perform pre-processing, analysis and template or atlas construction, however very few have been optimized for use with neonatal DTI data. Here we present a fully automated modular pipeline optimized for neonatal DTI data and the construction of study-specific tensor templates. We compare our methodology to an existing one. It is anticipated that the construction of population or study-specific templates will facilitate better group comparisons of neonatal populations both in health and disease.**

I. INTRODUCTION

Diffusion tensor imaging (DTI) enables the quantitative probing of cerebral white matter tracts and their microstructure in-vivo. The basic principle of DTI is to acquire a dataset containing a number of magnetic resonance imaging (MRI) volumes each with certain diffusion weighting in multiple directions. Processing of these datasets requires fitting a tensor model to quantify diffusion properties voxel-wise and derive metrics of the underlying microstructure that characterize the tensor shape, fractional anisotropy (FA), and tensor magnitude, mean diffusivity (MD) [1]. In order to perform group comparisons of these tensor maps and metrics between healthy and diseased populations proper normalization of each individual subject images in a common space is a known prerequisite. For this purpose rigid and non-rigid registration algorithms can be used to align and transform images from the individual subject's native image space to a common space, commonly referred to as a template or atlas. DTI based neonatal atlases and templates have been introduced by few groups. Oishi et al. [2] developed a multi-contrast neonatal brain atlas derived from DTI and co-registered anatomical MRI at 3.0T. Combined with a diffeomorphic transformation, they normalized 33 brain images from 22 healthy full-term newborns (ranging from 37 to 53 post-conceptional weeks), to the atlas space and parcellated it into 122 anatomical regions. They used their atlas to study developmental changes of the white matter across this age range. Finally, Terzopoulos et al. [3] created a template of 17 preterm infants without evidence of focal lesions on conventional MRI and 16 preterm infants both with and without evidence of brain injury. First, a T2-weighted template was reconstructed from structural MR images using an atlas building approach proposed by Seghers et al. [4] which has been successfully extended for building neonatal atlases [5]. Afterwards, resulting transformations were used to create FA and MD templates. Previous studies mentioned rely on the availability of of relatively high-contrast anatomical MR images to perform image registration used to create FA and MD templates. A methodology for building DTI based atlases exists (DTIAtlasBuilder) [6], however this is not optimized for neonatal DTI data. The purpose of this paper was to propose an optimized and automated yet robust DTI processing framework for neonatal DTI data that allows the construction of study-specific high resolution and high anatomical detail tensor templates to facilitate group comparisons.

*Supported by Canadian Institutes of Health Research (MOP-9116).

[1]Advanced Pediatric Brain Imaging Laboratory, Division of Diagnostic Imaging and Radiology, Children's National Medical Center, Washington, DC, 20010. ievangel@childrensnational.org

[2]Division of Fetal and Transitional Medicine, Children's National Medical Center, Washington, DC, 20010.

[3]Departments of Radiology and of Pediatrics, George Washington University School of Medicine and Health Sciences, Washington, DC, 20037.

II. METHODOLOGY

A. Subjects

This prospective study was approved by the local institutional review board and written informed consent was obtained from all study participants parents. Neonates were studied under natural sleep during MRI. They were fitted with ear protection and were secured in a vaccum-fixation device. They also had heart rate and oxygen saturation monitored during MRI. The healthy control cohort consisted of 27 neonates (18 males and 9 females), 38.96±1.45 gestational weeks at birth and 41.17±1.26 gestational weeks at MRI, and the patient cohort consisted of 43 neonates with congenital heart disease (24 males and 19 females) 38.07±1.39 gestational weeks at birth and 38.71±1.59 gestational weeks at MRI.

B. MRI Acquisition

All MRI scans were performed on an Achieva 1.5T MRI scanner (Philips Medical Systems, Best, Netherlands) and an 8-channel receive head coil. (In-Vivo Corp., Gainesville, FL). DTI scans were acquired using a single shot spin echo echoplanar imaging (EPI) sequence, repetition time, TR = 6600ms and echo time, TE = 100 ms, acquisition matrix = 128×128, voxel size 2.0x2.0x2.0mm^3, 3 signal averages, acceleration factor of 2, 1 volume with no diffusion weighting (b = 0) and 15 volumes in non-collinear gradient directions with diffusion weighting b = 700 s/mm^2. The scan time for the DTI acquisition was 5:23mins.

978-1-4244-7929-0/14/$26.00

C. DTI Processing

All raw data for all subjects were first organized per acquisition order and then converted to a 4D volume NIFTI file format from the scanner acquired DICOM format, using the `to3d` program, part of AFNI (http://afni.nimh.nih.gov/afni). The gradient table used was extracted from the DICOM headers. Subsequent steps included the quality inspection of the DTI data for artifacts originating from subject motion or scanner malfunction both visually and quantitatively.

1) Quality Inspection and Evaluation: For each 4D dataset the non-diffusion weighted volume is used to create a brain mask removing the skull and any extracranial tissue using the brain extraction tool, `bet2`, part of FSL (http://fsl.fmrib.ox.ac.uk/fsl/fslwiki/). The optimal values used for the fractional intensity threshold were 0.4 and for the vertical gradient in the fractional intensity threshold 0.2. The remaining diffusion weighted volumes, also with extracranial tissue removed, were used to calculate a quality index as 1 minus the Spearman (rank) correlation coefficient of each volume with the median volume. The acceptable range was defined as the range of the median -3.5×MAD to median +3.5×MAD where MAD is the Median Absolute Deviation defined as the median signal intensity of the absolute deviations from the median signal intensity [7]. Volumes outside this range were excluded as outliers from the 4D diffusion weighted dataset. The AFNI program `3dTqual` was used for this purpose and a sample output is shown in figure 1 below.

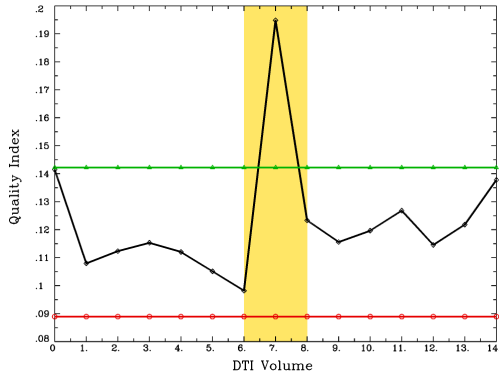

Fig. 1. Quality index per DTI volume, Median=0.116. In red -3.5×MAD=0.089 and in green +3.5×MAD=0.142. In yellow, the region flagged for being outside the acceptable range, (volume 7).

2) Pre-processing: The remaining diffusion weighted volumes were co-registered to the non-diffusion weighted volume (b=0) to correct for eddy-current induced distortions and movement related artifacts using 12 degrees of freedom affine registration with normalized mutual information as the cost function, using `flirt`, part of FSL. Then, the gradient vector table was rotated to account for the transformations that the dataset underwent during the motion and eddy current correction step [8]. The next step was to perform noise filtering of the DTI data while preserving their structure using anisotropic diffusion filtering implemented in AFNI as `3danisosmooth`. The optimal parameters used were gaussian smoothing σ = 0.2 before gradient matrix computation and gaussian smoothing σ = 0.5 after gradient matrix computation for calculation of structure tensor. Two iterations were a good compromise between adequate noise removal and blurring of the dataset. Finally, a tensor model was fitted voxel-wise with weighted least squares using `dtifit` from FSL. The tensor was decomposed in 3 pairs of eigenvalues and eigenvectors and the following DTI derived metrics were calculated, fractional anisotropy (FA), axial (AD), radial (RD) and mean diffusivity (MD). The processing steps are outlined in figure 2 below.

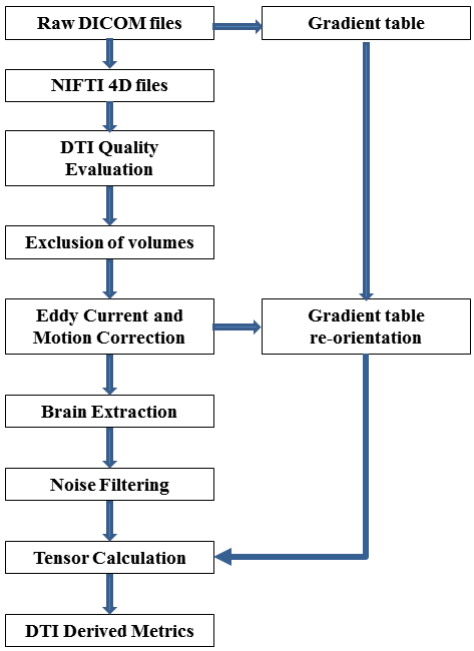

Fig. 2. DTI Pre-processing steps.

3) Tensor Template Construction: After all subject DTI data were processed and tensor maps were estimated, the template construction followed using algorithm 1 below. The optimal spatial normalization for an initial template was selected using a bootstrapping approach [9] from a subset of 5 subjects with relatively good visual alignment among them. Each subject's tensor map is registered to the average of all 5 tensor maps, by first rigid and then affine registration. The resulting bootstrapped template represents the initial template for all subsequent steps. Then each subject's tensor map was aligned to this initial template using affine registration and the square of the euclidean distance between tensors as the similarity function. This is an iterative process and the mean affine template was refined and re-generated 3 times. Using the final mean affine template as an initial step to the deformable registration process, each mean diffeomorphic template was refined 6 times in an iterative process. The final iteration provided the mean diffeomorphic template for each cohort is shown in figure 3 below.

All tensor registrations and the construction of the tensor templates were performed using DTI-TK [10] a non-parametric diffeomorphic deformable image registration that

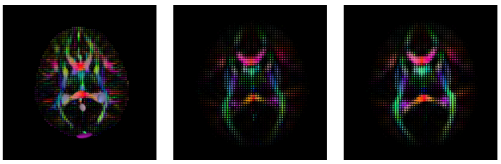

Fig. 3. Control Tensor template (a) Initial affine aligned template, (b) after 3 affine iterations, (c) after 6 iterations of deformable registration.

incrementally estimates the displacement field using a tensor-based registration formulation [11].

Algorithm 1: Tensor template construction

begin
  foreach *tensor* i **do**
    Convert from FSL eigensystem to NIFTI tensor
    Compute tensor norm $\|i\|$
    Convert diffusivity unit to mm$^2 s^{-1}$
    Remove outliers quantified with tensor norm $\|i\|$
    Convert tensor to symmetric and positive-definite
    Set tensor origin to [0 0 0]
  end
  Bootstrap *initial* template $\mathcal{T}^{init}$ from a subset of 5 subjects
  foreach *tensor* i **do**
    repeat
      Affine alignment to $\mathcal{T}^{init}$
    until $\mathcal{T}^{aff}_{iter} - \mathcal{T}^{aff}_{iter-1} < \delta$, *where* $\delta > 0$
  end
  Save final iteration to affine template $\mathcal{T}^{aff}$
  foreach *tensor* i **do**
    repeat
      Diffeomorphic registration to $\mathcal{T}^{aff}$
    until $\mathcal{T}^{diff}_{iter} - \mathcal{T}^{diff}_{iter-1} < \delta$, *where* $\delta > 0$
  end
  Save final iteration to diffeomorphic template $\mathcal{T}^{diff}$
end

III. RESULTS

To evaluate the accuracy and robustness of the templates constructed using the proposed methodology we constructed additional templates from our 2 cohorts using the existing DTI AtlasBuilder software tool [6]. We therefore, used a separate registration algorithm [12], to perform unbiased registrations to the templates constructed using both methodologies. The block matching algorithm for global registration `reg_aladin` was used to register each subject's FA map to each template. The symmetric version of the algorithm was used and a rigid transformation was performed followed by an affine with 12 degrees of freedom in 3 levels with 5 iterations per level. Using the final affine transformation as an initialization step a fast free-form deformation algorithm for non-rigid registration, `reg_f3d`, was used to to register each subject's FA map to each template [13]. The algorithm uses cubic b-spline to deform the source image in order to optimize a objective function based on the normalized mutual information similarity measure and bending energy as the penalty term in 3 levels and 300 iterations per level. The mean cross-correlation was computed between each subject's FA to the FA template constructed for each approach (table I). Only the FA templates were used since DTI AtlasBuilder uses the FA as the target image. The templates constructed using the proposed method demonstrated higher mean correlation between the template and each subject's FA than the templates constructed using DTIAtlasBuilder.

TABLE I
MEAN CROSS-CORRELATION (CC)

Atlas	Mean±SD
Proposed$_{controls}$	0.888±0.021
DTIAtlasBuilder$_{controls}$	0.783±0.026
Proposed$_{patients}$	0.888±0.021
DTIAtlasBuilder$_{patients}$	0.884±0.021

Furthermore, to evaluate the sharpness of the intensity in the constructed template we computed the variance of the registered intensity images to the respective templates. The voxel-wise intensity variance (IV) [14] of a population of N images i registered to template $\mathcal{T}_j$ is computed as

$$IV_j(\mathbf{x}) = \frac{1}{N-1}\sum_{i=1}^{N}\left(I_i(\mathbf{T}_{j,i}(\mathbf{x})) - \mathcal{T}_j(\mathbf{x})\right)^2 \qquad (1)$$

where $\mathbf{T}_{j,i}$ is the transformation from image i to template and $\mathcal{T}_j$ is the respective template image.

The templates constructed using the proposed method demonstrated lower mean intensity variance than the templates constructed using DTIAtlasBuilder (table II).

TABLE II
MEAN INTESITY VARIANCE (IV)

Atlas	Mean IV
Proposed$_{controls}$	0.006
DTIAtlasBuilder$_{controls}$	0.008
Proposed$_{patients}$	0.005
DTIAtlasBuilder$_{patients}$	0.004

The mean intensity variance images for the FA from the tensor templates for the 27 control neonates computed using equation (1) above, are shown in figure 4 below.

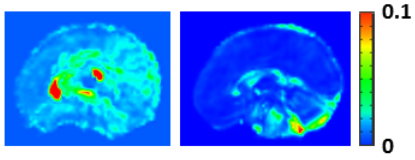

Fig. 4. Mid-sagittal slice of the mean intensity variance (IV) of the FA images showing higher variance across the whole brain (in green) and highest in the corpus callossum (in red) in the template created using DTI AtlasBuilder versus the mean intensity variance (IV) in the proposed template.

IV. DISCUSSION

Despite a number of challenges with the DTI acquisition of non sedated neonates, such as movement, vibration artifacts and low signal to noise, high quality tensor templates can be constructed (figure 5 below). One limitation is the absence of high-resolution T2-W anatomical images for this study which could be used to correct for geometric distortions occurring with the EPI sequence and drive the initial registrations.

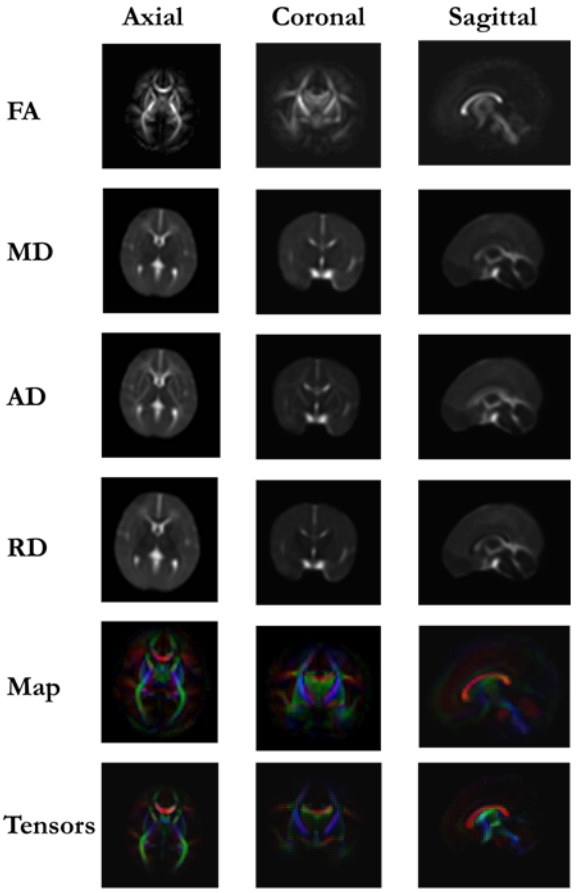

Fig. 5. Tensor template constructed from the 27 healthy control neonates and DTI derived metrics from this template.

The choice of using DTI-TK was well-suited for our study. As suggested by Wang et al. [15], DTI-TK showed the best performance and yielded best results among 8 software tools for DTI registration. They used scans of 10 age-matched neonates with infantile Krabbe disease mapped into an atlas for the analysis of major fiber tracts.

We constructed tensor templates for 27 healthy control neonates and 43 neonates with congenital heart disease that can be used to derive DTI metrics at the group level. These templates provide a higher resolution and superior anatomical detail than the atlases currently available. Despite our small sample size, the high quality of the template constructed allows for follow-up studies that use this methodology to create study specific templates rather than generic templates. Future work will focus on higher resolution acquisitions at 3.0T and whole brain tractography of the neonatal brain to study microstructural development in healthy and high-risk neonates.

REFERENCES

[1] P. J. Basser and C. Pierpaoli, Microstructural and physiological features of tissues elucidated by quantitative-diffusion-tensor MRI. *J Magn Reson*, 111(3):209-219, 1996.

[2] K. Oishi, S. Mori, P. K. Donohue, T. Ernst, L. Anderson, S. Buchthal, A. Faria, H. Jiang, X. Li, M. I. Miller, P. C. van Zijl, L. Chang. "Multi-contrast human neonatal brain atlas: application to normal neonate development analysis." *NeuroImage*, 56(1):8-20, 2011.

[3] V. Terzopoulos, H. C. Achterberg, A. Plaisier, A. M. Heemskerk, M. de Groot, D. Poot, W. J. Niessen, J. Dudink and S. Klein. "A 3D atlas of MR diffusion parameters in the neonatal brain," Perinatal and Pediatric Imaging (PaPI 2012), MICCAI Workshop, 73-80, 2012.

[4] D. Seghers, E. D'Agostino, F. Maes, D. Vandermeulen, P. Suetens, "Construction of a Brain Template from MR Images Using State-of-the-Art Registration and Segmentation Techniques", *MICCAI* , 696-703, 2004.

[5] A. Serag, P. Aljabar, G. Ball, S. J. Counsell, J. P. Boardman, M. A. Rutherford, A. D. Edwards, J. V. Hajnal, D. Rueckert, "Construction of a consistent high-definition spatio-temporal atlas of the developing brain using adaptive kernel regression", *NeuroImage*, 59(3), 2255-2265, 2012.

[6] A. R. Verde, J.B. Berger, A. Gupta, M. Farzinfar, A. Kaiser, et al. "UNC-Utah NA-MIC DTI framework: atlas based fiber tract analysis with application to a study of nicotine smoking addiction", *Proc. SPIE 8669, Medical Imaging 2013: Image Processing*, 86692D, March 13, 2013

[7] D. Pupert, "Statistics and Data Analysis for Financial Engineering," Springer Texts in Statistics, Springer, 2010.

[8] A. Leemans, and D. K. Jones, "The B-matrix must be rotated when correcting for subject motion in DTI data," *Magn Reson Med*, 61, 1336-1349, 2009.

[9] B. Efron, R. Tibshirani, "An Introduction to the Bootstrap". Boca Raton, FL: Chapman & Hall / CRC. 1993.

[10] H. Zhang, B. Avants, P. A. Yushkevich, J. H. Woo, S. Wang, L. H. McCluskey, L. B. Elman, E. R. Melhem, J. C. Gee, "High-dimensional spatial normalization of diffusion tensor images improves the detection of white matter differences in amyotrophic lateral sclerosis", *IEEE Trans on Med Imaging*, 26(11):1585-1597, 2007.

[11] H. Zhang, P. A. Yushkevich, D. C. Alexander and J. C. Gee, "Deformable registration of diffusion tensor MR images with explicit orientation optimization," *Med Imag Analysis*, 10, 764-785, 2006.

[12] S. Ourselin, A. Roche, G. Subsol, X. Pennec, N. Ayache, "Reconstructing a 3D structure from serial histological sections", *Image and Vision Computing*, 19(12):2531, 2001.

[13] M. Modat, G. R. Ridgway, Z. A. Taylor, M. Lehmann, J. Barnes, D. J. Hawkes, N. F ox, S. Ourselin. "Fast Free-Form Deformation using graphics processing units", *Comput Methods Programs Biomed*. Jun;98(3):278-84, 2010.

[14] G. E. Christensen, X. Introduction to the Non-Rigid Image Registration Evaluation Project (NIREP), *In J.P.W. Pluim, B. Likar, and F.A. Gerritsen (Eds.): WBIR*, LNCS 4057, pp. 128135, Springer-Verlag Berlin Heidelberg, 2006.

[15] Y. Wang, A. Gupta, Z. Liu, H. Zhang, M. L. Escolar, J. H. Gilmore, S. Gouttard, P. Fillard, E. Maltbie, G. Gerig, G. and M. Styner, "DTI registration in atlas based fiber analysis of infantile Krabbe disease," *NeuroImage*, 55, 1577-1586, 2011.